

Let's share CommRad: Co-existing Communications and Radar Systems

Narueporn Nartasilpa, Sara Shahi, Ahmad Salim,
Daniela Tuninetti, Natasha Devroye, and Danilo Erricolo
University of Illinois at Chicago, Chicago, IL 60607
Email: {nnarta2,sshahi,ahmads,danielat,devroye,derric1}@uic.edu

David P. Zilz, and Mark R. Bell
Purdue University, West Lafayette, IN 47907
Email: dzilz@purdue.edu, mrb@ecn.purdue.edu

Abstract—Spectrum sharing between radar and communications systems, as a means to address spectrum crunch, is an active research area. This paper considers Complex-valued Additive White Gaussian Noise (C-AWGN) communication systems co-existing with pulsed radar systems, and characterizes performance from two angles: 1) the effect of radar interference on a communications system is examined in terms of average error rate, constellation design, and Shannon capacity, and 2) the effect of communications interference on a radar system is examined in terms of the Receiver Operating Characteristic (ROC).

I. INTRODUCTION

Spectrum sharing between radar and communications systems has been a topic of interest as a potential solution to rapidly increasing demand for wireless spectrum. When both systems co-exist in the same spectrum, interference is unavoidable and some modifications to existing systems should be considered to account for the extra interference.

Several approaches to radar-communications spectrum sharing have been proposed in the open literature. For example, one straightforward interference mitigating solution is to split the available resources (in time or frequency) through policy so that each system operates independently and interference is avoided altogether. However, the two systems are limited to either accessing separate portions of the resources simultaneously or taking turns accessing the full resources. For example, a dynamic framework supporting needs-based resource distribution while enabling normal use of high performance cellular infrastructure was proposed in [1] so that each isolated user (with allocated bandwidth) can request multiple carriers so as to access larger instantaneous bandwidth. Another solution is to modify one system such that the performance degradation caused by interference is within a tolerable level. The authors in [2] presented a modified Wi-Fi receiver with an interleaver and a log-likelihood ratio mapping function, and two radar pulse detection approaches that can mitigate the radar interference. Much recent work has focused on the co-design of the coexisting radar-communications systems [3] (and references therein), with a particular focus on waveform design. Many of these waveform design problems utilize the characteristics of the other signal so as to improve each system's performance [4]–[7].

Before embarking in a full co-design, it is important to assess the performance of unaltered systems and understand

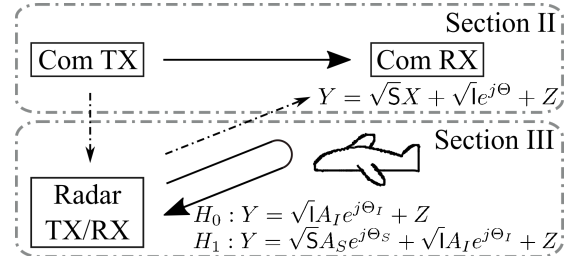


Figure 1: System diagram for co-existing systems.

what happens if the transmit sides of both systems are kept unaltered, which is the main focus of this work. These insights into the performance of unaltered systems can help guide future research directions in co-design synergies. This invited paper overviews the work of the Authors on the performance limits of unaltered co-existing and interfering communications and radar systems. The findings of this work are relevant for systems where changing the hardware may be too costly, but further digital signal processing of the baseband received signal is viable.

This paper investigates the performance limits of (separate and unaltered) radar and communications systems interfering with one another as shown in Figure 1. Our contributions are as follows. The error rate performance, the constellation design, and the Shannon capacity of a communications system in the presence of radar interference is presented in Section II. The detection performance of a radar system with interfering communications signals is presented in Section III. Section IV concludes the paper.

II. PERFORMANCE BOUNDS OF A COMMUNICATIONS SYSTEM CO-EXISTING WITH A RADAR SYSTEM

In this section, we first propose a model for radar interference to communications. We then investigate the error rate performance of a single-carrier communications system suffering from the radar interference and propose two constellation designs optimized for this particular system. Finally, we assess the error rate performance of a multi-carrier system.

A. On Modeling the Channel

Radar systems periodically transmit radar pulses of large amplitude and short duration while communications systems send signals of significantly lower power, smaller bandwidth,

and 100% duty-cycle. This implies that a narrowband communication system experiences the radar signal as an approximately amplitude-constant additive interference in the frequency domain. This amplitude can be accurately estimated from the knowledge of the slowly varying parameters of the radar waveform in the frequency domain. The phase, however, may change rapidly due to multipath propagation. It has been shown in [8] that the joint distribution of the radar amplitude and phase consists of a finite number of amplitudes, and conditioned on the amplitude the phase can be considered uniform. In general, one amplitude dominates the others, and the radar signal's joint distribution can be approximated by a uniform phase at that deterministic dominant amplitude. With these considerations in mind, we propose a simple model for two coexisting systems that captures some key performance bottlenecks and highlights various operating regimes.

B. Single-Carrier Communications Systems

In this section, for single-carrier communications systems interfered by a radar signal, we first derive the Symbol Error Rate (SER) for optimal and suboptimal detectors, and then we present optimal signal constellation designs subject to two different criteria: (a) to maximize the transmission rate under a power budget and an SER constraint, and (b) to minimize the SER under a power constraint and a fixed rate condition. We conclude with the characterization of the Shannon capacity.

The discrete-time complex-valued received signal at the communications receiver with pulsed radar interference is

$$Y = \sqrt{S}X + \sqrt{I}e^{j\Theta} + Z, \quad (1)$$

where S is the average Signal-to-Noise Ratio (SNR) of the communications signal, X is the equally-likely unit-energy complex-valued transmitted symbol from the constellation $\mathcal{X} = \{x_1, \dots, x_M\}$ of size M , I is the Interference-to-Noise Ratio (INR) of the radar signal, Θ is the radar phase uniform in $[0, 2\pi)$, and Z is a zero-mean unit-variance proper-complex Gaussian noise. The random variables (X, Θ, Z) are mutually independent and the pair (S, I) is known and fixed.

Optimal Decoder: The likelihood function for the received signal in (1) is given by the Rice-like distribution

$$f_{Y|X}(y|x) = \mathbb{E}_{\Theta \sim \mathcal{U}[0, 2\pi]} \left[\frac{1}{\pi} e^{-|y - \sqrt{S}x - \sqrt{I}e^{j\Theta}|^2} \right]. \quad (2)$$

The optimal Maximum Likelihood (ML) receiver chooses the following estimate of the transmitted symbol [9, Eq.(2)]

$$\hat{x}^{(\text{OPT})}(y) := \arg \min_{x \in \mathcal{X}} |y - \sqrt{S}x|^2 - \ln I_0(2\sqrt{I}|y - \sqrt{S}x|), \quad (3)$$

where I_0 denotes the modified Bessel function of the first kind of order zero. We can approximate the ML receiver in (3) in two regimes (weak and strong radar interference) as follows.

Suboptimal Decoders: When $I \ll S$, we have $I_0(z) \cong 1$ for $|z| \ll 1$ [10, Eq.(9.6.12)], and thus the receiver in (3) chooses an estimate

$$\hat{x}^{(\text{OPT})}(y) \approx \hat{x}^{(\text{TIN})}(y) := \arg \min_{x \in \mathcal{X}} |y - \sqrt{S}x|^2. \quad (4)$$

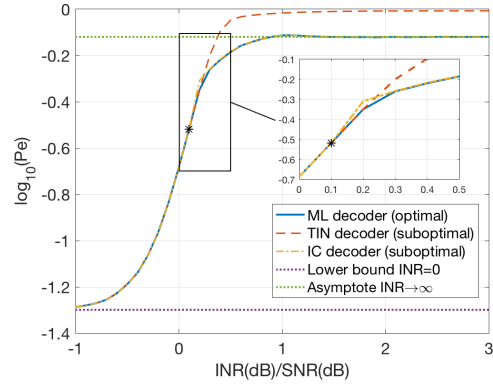


Figure 2: SERs of all decoders for a 64-QAM at $S = 20$ dB.

That is, weak radar interference is treated as Gaussian noise. The receiver in (4) is referred to as the Treat Interference as Noise (TIN) decoder and its SER at low INR [11, Eq.(16)] is

$$P_e^{(\text{OPT})} \leq P_e^{(\text{TIN})} = \frac{1}{M} \sum_{\ell=1}^M \mathbb{E}_{\Theta} \left[Q \left(\sqrt{\frac{Sd_{\min}^2}{2}} - \sqrt{2I} \cos(\Theta) \right) \right], \quad (5)$$

where $d_{\min} = \min_{k:k \neq \ell} |x_k - x_{\ell}|$ is the minimum Euclidean distance between the constellation symbols.

When $I \gg S$, we have $I_0(z) \cong e^{|z|}$ for $|z| \gg 1$ [10, Eq.(9.7.1)], and thus the receiver in (3) chooses an estimate

$$\hat{x}^{(\text{OPT})}(y) \approx \hat{x}^{(\text{IC})}(y) := \arg \min_{x \in \mathcal{X}} (|y - \sqrt{S}x| - \sqrt{I})^2 \quad (6)$$

$$= \arg \min_{x \in \mathcal{X}} (\Re\{e^{-j\Theta}(y - \sqrt{I}e^{j\Theta} - \sqrt{S}x)\})^2. \quad (7)$$

The expression in (6) implies that the receiver attempts to cancel the radar interference; in doing so, part of the communications signal is also cancelled, and the channel reduces to a real-valued phase-fading Gaussian channel as in (7). The receiver in (7) is referred to as the Interference Cancellation (IC) decoder and its SER at high INR [11, Eq.(21)] is

$$P_e^{(\text{OPT})} \leq P_e^{(\text{IC})} \approx \frac{1}{M} \sum_{\ell=1}^M \mathbb{E}_{\Theta} \left[Q \left(\min_{\substack{k \neq \ell: \\ \text{sign}(r_k - r_{\ell}) \geq 0}} \sqrt{\frac{S}{2}} |r_k - r_{\ell}| \right) + Q \left(\min_{\substack{k \neq \ell: \\ \text{sign}(r_k - r_{\ell}) < 0}} \sqrt{\frac{S}{2}} |r_k - r_{\ell}| \right) \right], \quad (8)$$

Figure 2 plots the SER vs normalized INR in dB for the 64-QAM constellation at $S = 20$ dB. It shows that the SER of the TIN and IC decoders in (5) and (8), respectively, yield fairly tight upper bounds on the SER of the optimal ML decoder in (3). The SER increases with I in the low INR regime and reaches its highest at $I \approx S$, then it slightly decreases but does not become $1 - 1/M \approx 10^{-0.0068}$ since the radar interference can be canceled. Similar observations hold for all S 's and all constellations. Notice that all three decoders exhibit the same SER curves at low INR up to $I_{\text{dB}} = 0.1S_{\text{dB}} = 2$, marked by *.

Given that the channel with weak radar interference in (4) still behaves as an AWGN channel, commonly-used modulation schemes designed for the AWGN-only channel such as

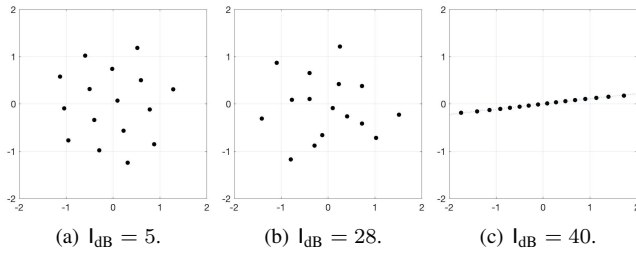


Figure 3: Designed constellations that minimize the SER in (9) at $S_{dB} = 20$ and $l_{dB} = 0.25S_{dB}, 1.4S_{dB}$ and $2S_{dB}$ for $M = 16$.

QAM and PSK can still be used. However, those constellations might not be suitable for the real-valued phase-fading channel when the radar interference is strong as in (7). Thus, we present next two constellation design approaches.

Constellation Design for Minimizing the Error Rate: The constellation yielding the lowest error rate subject to fixed constellation size M and power constraints is formulated as

$$P_e^{(OPT)}(M) = \min_{\mathcal{X}} P_e(\mathcal{X}) \quad (9a)$$

$$\text{s.t. } \mathbb{E}_{X \in \mathcal{X}}[|X|^2] \leq 1, |\mathcal{X}| = M, \quad (9b)$$

where $P_e(\mathcal{X})$ is the SER of the ML receiver for constellation \mathcal{X} . As there is no closed-form for the optimal SER, we use its approximations in (5) at low INR and (8) at high INR in (9) to optimize the location of the equally-likely constellation points.

Constellation Design for Maximizing the Transmission Rate: Given constraints on the power and SER, the optimization problem for the constellation with largest cardinality is

$$M^{(OPT)}(\varepsilon) = \max_{\mathcal{X}} |\mathcal{X}| \quad (10a)$$

$$\text{s.t. } \mathbb{E}_{X \in \mathcal{X}}[|X|^2] \leq 1, P_e(\mathcal{X}) \leq \varepsilon. \quad (10b)$$

Figure 3 shows the SER-minimized designed constellations for $M = 16$ at $S = 20$ dB and $l = 5, 28, 40$ dB, representing low, middle and high INR regimes, respectively. The designed constellation is shaped as a concentric hexagon for $l \ll S$, and morphs into an unequally-spaced PAM for $l \gg S$. At high INR, one of the two real-valued dimensions is lost. Thus, it makes intuitive sense that the points are placed along one dimension.

The constellations in Figure 3, compared to classical ones, yield the lowest error rates at all INR ranges, though PAM is quite competitive at high INR, as it can be observed in Figure 4. This actually suggests that when a communications system is interfered by a strong radar signal, it is not necessary to design a constellation as PAM is sufficient when using the IC decoder. The shapes of the designed constellations maximizing the transmission rates are the same as the ones minimizing the error rates, as seen in [12, Table II and III]. Note that even though PAM achieves comparable maximum transmission rate as the (designed) uneven PAM at high INR, the uneven PAM still outperforms PAM at high SNR.

Shannon Capacity: The insights that emerged from the performance analysis of uncoded communications systems align with those obtained when considering the Shannon capacity of the channel model in (1).

The capacity achieving input distribution for this channel

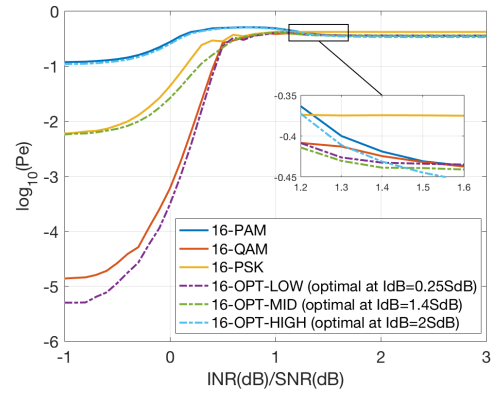


Figure 4: SER Comparison of the SER-minimized designed constellations with classical ones for $M = 16$ and $S = 20$ dB.

has independent modulo and phase, where the phase is uniformly distributed in $[0, 2\pi)$ in [13]. The modulo is, however, discrete with countably infinite many mass points but only finitely many of them in any bounded interval. Hence, finding the exact weight and location of the modulo mass points corresponds to an infinite dimensional optimization problem. Numerical evaluations [13, Section V] show that the capacity can be well approximated by restricting the cardinality of the amplitude mass points to some finite value that should increase with the SNR. Also, a Gaussian distribution well approximates the capacity, both in weak and strong radar interference regimes [13, Section V]. Moreover, at high INR, in agreement with (7), the capacity is equal to a half of the interference-free complex-valued channel capacity, i.e. $\frac{1}{2} \log(1 + S)$, and a Gaussian distributed input achieves it [13, Theorem 2].

C. Multi-Carrier Communications System

OFDM-based systems have been widely used in current high speed networks unlike narrowband single-carrier systems as presented previously. Here we consider a general OFDM communications system of N subcarriers and L OFDM blocks with additive white Gaussian noise and radar interference.

In [12], we assumed that the OFDM receiver samples at the sampling period of T_S in synchrony with the transmitted symbols, and the radar signal arrives *randomly* at the receiver T_d seconds after the communications signal. The unknown time delay T_d is modeled as uniformly distributed and causes the received signal to be correlated in both time and frequency. The optimal ML receiver decodes N subcarriers and L blocks altogether. Suboptimal receivers are categorized based on what correlation in the received signal is leveraged: the `subtime` decoder considers only the correlation in time; the `subfreq` decoder considers the correlation in frequency only; and the `subnone` decoder considers the received signal as uncorrelated (symbol-by-symbol detector). The detailed channel model is not reported here for sake of space, but can be found in [12, Section III]. Note that fading was not considered.

The performance of the receivers in terms of Block Error Rate (BLER) and SER are given by [12, Eq.(35)-(37)], which are evaluated via Monte Carlo simulation. Numerical results concluded that the `subfreq` decoder generally performs

slightly better than the `subnone` decoder but it does not perform as well as the `subtime` decoder. This indicates that accounting for time correlation (i.e. decoding several OFDM blocks at once at the expense of increased complexity) is critical for good performance. The use of the `subtime` decoder is recommended if the computation time is a major constraint since the computation time of the optimal decoder increases with the constellation size. Note that the error rates increase with the constellation size, and an increase in the radar pulse width degrades the performance of the system.

D. Conclusions and Future Work

The error rate analysis showed that a single-carrier communications receiver should treat the radar interference of weak power as Gaussian noise, while the receiver should estimate the radar interference of strong power and cancel it. The latter, however, causes a loss of half the degrees of freedom. The constellation designed by either minimizing the error rate or maximizing the transmission rate tends to a hexagonal shape in the weak radar regime, while it tends to an unevenly-spaced PAM in the opposite regime. The received signal at a multi-carrier OFDM communications receiver is correlated in both time and frequency due to the unknown time lag between radar and communications signals. The suboptimal decoders are categorized into three types based on the correlation. Numerical evaluations showed that the suboptimal time-correlated receiver yields the lowest error rate (slightly lower than the optimal one) among all the suboptimal receivers. How these results change in the presence of coded systems is an interesting area of future work.

III. PERFORMANCE BOUNDS OF A RADAR SYSTEM CO-EXISTING WITH A COMMUNICATIONS SYSTEM

In this section, we consider the performance of a radar system in the presence of interfering communications signals, the complementary aspect of the analysis in Section II. We first propose a statistical model for communications interference to radar, motivated by existing theoretical models and supported by original simulations. We then assess the impact of communications interference on the probabilities of false alarm and detection for a cell-averaging adaptive-threshold radar detector—which is known to have a Constant False Alarm Rate (CFAR) in AWGN only. Our results suggest potential strategies for improving radar detection in the presence of communications interference for future work.

A. On Modeling the Channel

A statistical distribution for the interference must be specified to model the effects of communications interference on radar detection. Thus, we examine existing theoretical interference models before turning toward original simulations.

Theoretically, while some spectrum sharing studies (cf. [2]) assume a Gaussian model for communications interference to radar, non-Gaussian models also have theoretical justification in some scenarios. Theoretically justified non-Gaussian interference models include the spherically invariant models

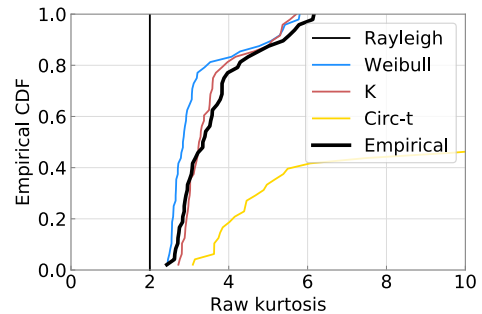


Figure 5: Empirical kurtosis of simulated interference, compared with kurtosis of four fitted models, for the case of single-user OFDM with slow Rician fading and fixed location and path loss.

of [14], the alpha-stable models of [15], and the models developed by Middleton in [16]. In addition, we have conducted empirical simulation studies of wireless communications interference [17], and these also suggest both Gaussian and non-Gaussian interference statistics, depending on the situation. In our simulations, we assume perfect alignment of radar and communications carrier frequencies. We generate random OFDM communications signals, apply Rician fading, apply a path loss model of $(1+r)^{-\nu}$ as a function of radial distance r (where $\nu \geq 1$ is a path loss exponent depending on the particular propagation environment), sum the results, and pass the composite received interference through a linear frequency modulated (LFM) radar matched filter. Some example statistical results are presented in Figure 5. As shown in this figure, the compounding effects of OFDM signaling and slow Rician fading lead to heavy-tailed statistics at the output of the matched filter, which are well modeled by the K distribution. Further, in other results we observe that when the locations of the communications transmitters are randomized (and hence path loss via the path loss function $(1+r)^{-\nu}$), even more heavy-tailed statistics can result. In general, we find that non-Gaussian statistics may result from averaging over random wireless channel and network effects, such as multipath fading, transmitter motion, and transmitters turning ON and OFF.

In conclusion, we propose the following Probability Density Function (PDF) for the magnitude A_I of the interference output of the radar matched filter:

$$f_{A_I}(a) = (1-p)\delta(a) + p \frac{4}{\lambda \Gamma(\alpha)} \left(\frac{a}{\lambda}\right)^\alpha K_{\alpha-1}\left(\frac{2a}{\lambda}\right) 1_{[0,\infty)}(a), \quad (11)$$

where p , α , and λ are parameters of the distribution, $\delta(\cdot)$ is the Dirac delta function, $\Gamma(\cdot)$ is the Gamma function, $K_\nu(\cdot)$ is a modified Bessel function of the second kind, and the indicator function equals one for non-negative values of its argument and zero otherwise. This model subsumes several Gaussian and non-Gaussian models as special cases.

B. Radar Receiver Operating Characteristic (ROC)

Using the statistical model (11) for wireless communications interference described in the previous section, we assess the impact of such interference on radar detection.

Specifically, we compute the probability of false alarm (P_{FA}) and probability of detection (P_D) for a cell-averaging adaptive-threshold radar detector operating in communications interference modeled by (11).¹ The cell-averaging adaptive-threshold detector makes decisions about whether a target is present (H_1) or not (H_0) by comparing the matched filter output Y in the delay-Doppler cell-under-test (CUT) with a threshold set adaptively based on the sample average energy in the matched filter outputs Y_1, \dots, Y_N in N neighboring delay-Doppler cells:

$$\phi(y) = \begin{cases} 1, & |y|^2 > \tau \frac{1}{N} \sum_{n=1}^N |Y_n|^2, \\ 0, & |y|^2 \leq \tau \frac{1}{N} \sum_{n=1}^N |Y_n|^2, \end{cases} \quad (12)$$

where τ is a design parameter related to the probability of false alarm P_{FA} in AWGN only.

In (12), we model the $N + 1$ matched filter outputs Y, Y_1, \dots, Y_N as

$$Y_n = \sqrt{I} A_{I,n} e^{j\Theta_{I,n}} + Z_n, \text{ for } n = 1, \dots, N, \quad (13)$$

$$Y = \begin{cases} \sqrt{I} A_I e^{j\Theta_I} + Z, & \text{under } H_0, \\ \sqrt{S} e^{j\Theta_S} + \sqrt{I} A_I e^{j\Theta_I} + Z, & \text{under } H_1, \end{cases} \quad (14)$$

where S is the SNR; Θ_S is a random signal phase uniform on $[0, 2\pi)$; I is the mean INR (“mean” since the interference is modeled as random); $A_I, A_{I,1}, \dots, A_{I,N}$ are random interference amplitudes distributed according to (11), with λ set so that $E[A_I^2] = 1$; $\Theta_I, \Theta_{I,1}, \dots, \Theta_{I,N}$ are random interference phases uniform on $[0, 2\pi)$; and Z, Z_1, \dots, Z_N are i.i.d. circular Gaussian noise terms with mean-square of unity. Finally, although in general the interference amplitudes $A_I, A_{I,1}, \dots, A_{I,N}$ and phases $\Theta_I, \Theta_{I,1}, \dots, \Theta_{I,N}$ could have an arbitrary joint statistical behavior, for the sake of analytical tractability we qualitatively bound this joint behavior using the two extreme cases of: (i) One random realization of $A_I = A_{I,1} = \dots = A_{I,N}$ and $\Theta_I = \Theta_{I,1} = \dots = \Theta_{I,N}$ across all delay-Doppler cells (“slow” interference), and (ii) $N + 1$ i.i.d. realizations of both the amplitude and phase across all cells (“fast” interference).

Based on this statistical model for the cell-averaging radar detector (12), we compute its probability of false alarm $P_{FA} = E[\phi(Y)|H_0]$ and probability of detection $P_D = E[\phi(Y)|H_1]$, in order to assess how its detection performance varies with the statistical characteristics of the interference. The details of this derivation are presented in [17], and the complete set of computed results is available in [18]. Here we simply summarize the primary findings. Communications interference impacts the cell-averaging radar detector (12) via two types of mechanisms: (i) Model mismatch, and (ii) Boost in the background noise level. We discuss each of these in turn.

Model mismatch: The cell-averaging detector (12) is designed to maintain CFAR, assuming that any background noise, clutter, and interference is well modeled as AWGN.

¹ Adaptive-threshold radar detectors such as this adjust a detection threshold adaptively to maintain a steady false alarm rate, even when noise levels are fluctuating.

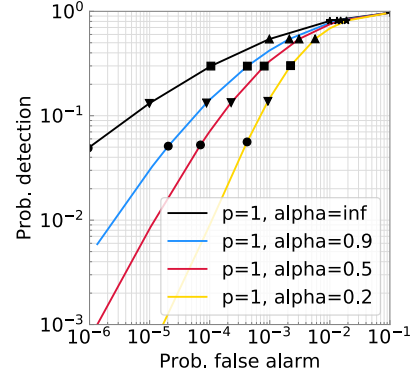


Figure 6: P_D versus P_{FA} for the radar detector (12) with “fast,” heavy-tailed interference ($p = 1$ and $\alpha < \infty$ in (11)) for $S = 10$ dB, $I = -5$ dB, and $N = 32$ cells.

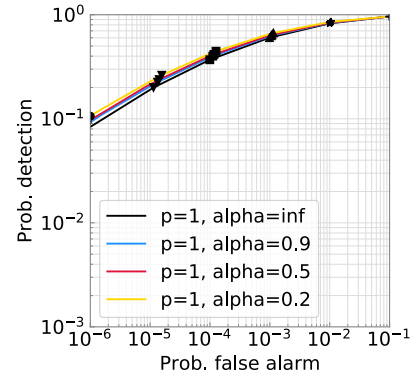


Figure 7: P_D versus P_{FA} for the radar detector (12) with “slow,” heavy-tailed interference ($p = 1$ and $\alpha < \infty$ in (11)) for $S = 10$ dB, $I = -5$ dB, and $N = 32$ cells.

When the AWGN assumption is violated, through either non-Gaussian statistics or non-white correlation in time, unexpected detection behavior can result.

The effects of *non-Gaussian* interference on radar detection are illustrated in Figure 6. This figure shows the P_D - P_{FA} curves for three non-Gaussian distributions (11) compared with a Gaussian distribution with equivalent mean INR. In Figures 6–7, each marker style corresponds to a fixed choice of the scalar τ in (12) and indicates the drift in operating point caused by violation of the Gaussian assumption.² As can be seen in the figure, heavy-tailed non-Gaussian interference can cause dramatic increases to the probability of false alarm P_{FA} relative to Gaussian interference with equivalent mean INR.

The effects of *non-white* interference on radar detection are illustrated via the contrast between Figures 6 and 7, the former corresponding to “fast” (white) interference, and the latter to “slow” interference. In the specific calculations plotted in Figures 6–7, notice that the deleterious effects of interference are tempered by the slow coherence time of the interference in the latter figure relative to the former. In any case, the

²For example, if one had set τ to achieve a probability of false alarm $P_{FA} = 10^{-5}$ under Gaussian interference, under heavy-tailed interference with $\alpha = 0.2$, one actually observes a probability of false alarm $P_{FA} \approx 10^{-3}$, as shown by the triangular markers in Figure 6.

response of the detector can vary significantly depending on the coherence time of the interference.

Boost in the background noise level: Even when wireless communications interference is well modeled as AWGN, it still increases the background noise level, and this can cause significant and insidious detection losses, even at relatively low INR (e.g. about -6 to -2 dB mean INR at the output of the matched filter) (cf. [18]). This phenomenon is reminiscent of results obtained experimentally by NTIA in [19], although we note that potentially different system configurations and definitions of INR make direct comparison difficult.

C. Conclusions and Future Work

Thus, both Gaussian and non-Gaussian statistical models may describe wireless communications interference, depending on the modeling situation. When interference is not well modeled as AWGN, mean INR is insufficient to characterize interference effects on the cell-averaging radar detector, and additional interference characteristics such as kurtosis/impulsiveness and coherence time also impact radar detection performance. Finally, communications interference increases the background noise level, and this can cause significant, insidious detection losses at relatively low INR.

Future work should examine innovative ways to improve radar detection in the presence of wireless communications interference. For example, when communications interference is non-Gaussian, innovative adaptive thresholds (cf. [20]) and non-linear alternatives to the matched filter (cf. [14], [21]–[23]) may improve radar detection performance. In addition, two of the Authors have submitted work for IEEE publication that uses linear, periodically time-varying (LPTV) filtering to effectively cancel a certain class of digital communications interference to radar.

IV. CONCLUSIONS

This paper overviews known bounds on the performance of an unaltered communications system interfering with a radar system, and vice versa. These results will be used to benchmark the performance of actual co-design schemes, where both systems are altered in order to facilitate spectrum sharing. Moreover, such co-designs – in which the communications and radar performance metrics should have well defined operational meanings – will have to be compared with the ultimate (Shannon-like) limits of co-existing systems such as that initiated in [3]. This research was supported by the National Science Foundation under the Enhancing Access to Radio Spectrum (EARS) program, grant award number 1443967 and 1443971. The contents of this article are solely the responsibility of the Authors and do not necessarily represent the official views of the NSF.

REFERENCES

[1] H. Shajiaah, A. Khawar, A. Abdel-Hadi, and T. C. Clancy, “Resource allocation with carrier aggregation in LTE advanced cellular system sharing spectrum with s-band radar,” in *IEEE International Symposium on Dynamic Spectrum Access Networks (DYSPAN)*, Apr. 2014, pp. 34–37.

[2] M. Mehrnoush and S. Roy, “Coexistence of WLAN network with radar: Detection and interference mitigation,” *IEEE Transactions on Cognitive Communications and Networking*, vol. 3, no. 4, pp. 655–667, Dec. 2017.

[3] A. R. Chiriyath, B. Paul, and D. W. Bliss, “Simultaneous radar detection and communications performance with clutter mitigation,” in *Proc. of IEEE Radar Conference (RadarConf)*, Seattle, WA, May 2017.

[4] M. J. Nowak, Z. Zhang, Y. Qu, D. A. Dessources, M. Wicks, and Z. Wu, “Co-designed radar-communication using linear frequency modulation waveform,” in *Proc. of IEEE Military Communications Conference (MILCOM)*, Baltimore, MD, Nov. 2017.

[5] Y. Zhang, Q. Li, L. Huang, C. Pan, and J. Song, “A modified waveform design for radar-communication integration based on LFM-CPM,” in *IEEE 85th Vehicular Technology Conference (VTC Spring)*, Sydney, Australia, Jun. 2017.

[6] W.-Q. Wang, Z. Zheng, and S. Zhang, “OFDM chirp waveform diversity for co-designed radar-communication system,” in *18th International Radar Symposium (IRS)*, Prague, Czech Republic, Jun. 2017.

[7] C. Sahin, J. Jakabosky, P. M. McCormick, J. G. Metcalf, and S. D. Blunt, “A novel approach for embedding communication symbols into physical radar waveforms,” in *Proc. of IEEE Radar Conference (RadarConf)*, Seattle, WA, May 2017.

[8] A. Salim, D. Tuninetti, N. Devroye, and D. Erricolo, “Modeling the interference of pulsed radar signals in OFDM-based communication systems,” in *Proc. of IEEE Radar Conference (RadarConf)*, Seattle, WA, May 2017.

[9] N. Nartasilpa, D. Tuninetti, N. Devroye, and D. Erricolo, “Let’s share CommRad: effect of radar interference on an uncoded data communication system,” in *Proc. of IEEE Radar Conference (RadarConf)*, Philadelphia, PA, May 2016, pp. 1–5.

[10] M. Abramovitz and I. A. Stegun, *Handbook of Mathematical Functions*. New York: Dover Publications, Inc, 1970.

[11] N. Nartasilpa, D. Tuninetti, N. Devroye, and D. Erricolo, “On the error rate of a communication system suffering from additive radar interference,” in *Proc. of IEEE Global Communication Conference (GlobeCom)*, Washington, DC, Dec 2016.

[12] N. Nartasilpa, A. Salim, D. Tuninetti, and N. Devroye, “Communications system performance and design in the presence of radar interference,” *submitted to IEEE Transactions on Communications*, 2017.

[13] S. Shahi, D. Tuninetti, and N. Devroye, “On the capacity of the AWGN channel with additive radar interference,” *IEEE Transactions on Communications*, Oct 2017.

[14] K. Sangston and K. Gerlach, “Coherent Detection of Radar Targets in a Non-Gaussian Background,” *IEEE Transactions on Aerospace and Electronic Systems*, vol. 30, no. 2, pp. 330–340, Apr. 1994.

[15] M. Haenggi and R. K. Ganti, “Interference in Large Wireless Networks,” *Foundations and Trends in Networking*, vol. 3, no. 2, pp. 127–248, 2008.

[16] D. Middleton, “Statistical-Physical Models of Electromagnetic Interference,” *IEEE Transactions on Electromagnetic Compatibility*, vol. EMC-19, no. 3, pp. 106–127, Aug. 1977.

[17] D. P. Zilz and M. R. Bell, “Statistical Modeling of Wireless Communications Interference and Its Effects on Adaptive-Threshold Radar Detection,” *Accepted for publication in IEEE Transactions on Aerospace and Electronic Systems*, 2017.

[18] —, “Statistical Results on the Performance of an Adaptive-Threshold Radar Detector in the Presence of Wireless Communications Interference,” Purdue University, Department of Electrical and Computer Engineering Technical Reports, Paper 482, Tech. Rep., Oct. 2017. [Online]. Available: <http://docs.lib.purdue.edu/ecetr/482/>

[19] F. H. Sanders, “Effects of RF Interference on Radar Receivers,” NTIA Report TR-06-444, Tech. Rep., Feb. 2006.

[20] P. Weber and S. Haykin, “Ordered Statistic CFAR Processing for Two-Parameter Distributions with Variable Skewness,” *IEEE Transactions on Aerospace and Electronic Systems*, vol. AES-21, no. 6, pp. 819–821, Nov. 1985.

[21] S. A. Kassam, *Signal Detection in Non-Gaussian Noise*. New York, NY: Springer-Verlag, 1988.

[22] E. Conte, M. Lops, and G. Ricci, “Asymptotically Optimum Radar Detection in Compound-Gaussian Clutter,” *IEEE Transactions on Aerospace and Electronic Systems*, vol. 31, pp. 617–625, Apr. 1995.

[23] S. Kraut, L. Scharf, and L. McWhorter, “Adaptive Subspace Detectors,” *IEEE Transactions on Signal Processing*, vol. 49, no. 1, pp. 1–16, 2001.